AIP | Applied Physics Letters

Optical electrical current sensor utilizing a graphene-microfiber-integrated coil resonator

Shao-cheng Yan, Bi-cai Zheng, Jin-hui Chen, Fei Xu, and Yan-qing Lu

Citation: Applied Physics Letters **107**, 053502 (2015); doi: 10.1063/1.4928247
View online: http://dx.doi.org/10.1063/1.4928247
View Table of Contents: http://scitation.aip.org/content/aip/journal/apl/107/5?ver=pdfcov
Published by the AIP Publishing

Optical electrical current sensor utilizing a graphene-microfiber-integrated coil resonator

Shao-cheng Yan, Bi-cai Zheng, Jin-hui Chen, Fei Xu,[a] and Yan-qing Lu
National Laboratory of Solid State Microstructures, Collaborative Innovation Center of Advanced Microstructures, and College of Engineering and Applied Sciences, Nanjing University, Nanjing 210093, People's Republic of China

(Received 15 March 2015; accepted 28 July 2015; published online 4 August 2015)

A graphene-based electrical current sensor is proposed utilizing a microfiber coil resonator. Monolayer graphene sheet with a large sheet resistance is transferred onto the surface of a glass capillary rod. A microfiber is spirally wrapped around the graphene sheet to form a coil resonator. Heat generated from electrical current shifts the resonant wavelength because of the thermal effect in the microfiber resonator. The sensor exhibits a very good performance with a high sensitivity of 67.297 $\mu m/A^2$, which is two orders of magnitude higher than that reported earlier. Our results show that microfiber-graphene-integrated devices have great potential for miniature and highly sensitive fiber sensors for monitoring electrical current. © *2015 AIP Publishing LLC*.
[http://dx.doi.org/10.1063/1.4928247]

Optical fiber sensors have been extensively studied for several superior performances, including immunity to electromagnetic interference, electrical isolation, high sensitivity, light weight, and ease to connect to other fiber devices, compared with traditional sensors.[1] A considerable number of electrical current sensors have been developed utilizing different optical fiber structures such as fiber interferometers, gratings, lasers, and resonators. They are mainly divided into several categories, for example, Faraday effect,[2–4] Ampere force,[5] thermal effect,[6–13] etc. The first kind of current sensors is limited by small Verdet constant of optical fiber material and needs a large number of coils to gain a large sensitivity and polarization dependent manipulation. The second type needs a pre-placed magnetic field to realize electrical current sensing, which makes the system more complicated. Current sensors based on the thermal effect are attractive if the short response-time is not so important, because they can be assembled easily with a very high sensitivity. In order to acquire a high sensitivity, a high-resistance metal bar and a small volume fiber configuration are preferred. Subwavelength-diameter microfiber is an ideal element for miniature fiber devices, and various microfiber-based electrical current sensors have been demonstrated by binding microfibers to metal rods or metal films whose resistances are still limited by the thickness.

Meanwhile, metalloid graphene has attracted more and more interest because of many extraordinary electrical, mechanical, and optical properties. Graphene is a two-dimensional one-atom-thick sheet where carbon atoms are configured in a honeycomb lattice.[14] It is the most promising candidate for future high-speed electronic applications due to high carrier mobility and large saturation velocity. Chemical vapor deposition (CVD) techniques have been applied to grow high quality monolayer graphene sheet on the metal substrate, such as Cu, Pt, and Ir.[15] Based on its unique properties, such as high surface area and high mechanical strength, devices have been designed for purposes of electrochemical and bio-sensing, taking advantage of electrical properties of graphene.[16,17] However, no many optical sensors have been proposed, especially electrical current sensors utilizing optical fiber structures. In fact, monolayer graphene has a large sheet resistance and is perfect for fiber-optic based electrical current sensors based on thermal effect. Metal films can provide a large sheet resistance, which is also applicable to the sensor. However, to get an analogous large resistance and other performance, the thickness of metal films needs to be reduced to a similar level with graphene,[18] and it is challenging to coat one-atom thick film uniformly on a cylindrical rod and expensive vacuum-coating technology has to be employed. In contrast, graphene is relatively cheaper, and transferring process is much easier.

In this work, we take advantage of the property of large sheet resistance to realize optical sensing of electrical current. With the lab-on-a-rod technique, we coat a glass capillary rod with a monolayer graphene sheet, and spirally wrap a microfiber around the graphene sheet to form an optical coil resonator.[19–21] Based on the graphene-microfiber-integrated device, we demonstrate an electrical current sensor with an ultra-high sensitivity of ~67.297 $\mu m/A^2$, which is two orders of magnitude higher than current sensors based on thermal effect publishedearlier.[9–13] The fabrication process is reliable and permits easy handling. The device is compact and stable.

Figure 1(a) shows the schematic diagram of our electrical current sensor, which is fabricated by wrapping a microfiber around a glass capillary rod coated by a monolayer graphene sheet. First, we fabricate a microfiber with the so-called flame brushing method.[22] The single-mode fiber (SMF-28, Corning, USA) is heated and tapered to the microfiber with specific diameter by controlling the stretching speed. The microfiber contains a uniform waist region, two transition regions, and two pigtails. To acquire the sample, a small piece of monolayer graphene sheet on the copper substrate is tailored carefully in advance and spin-coated with the polymethyl methacrylate

[a]Electronic mail: feixu@nju.edu.cn.

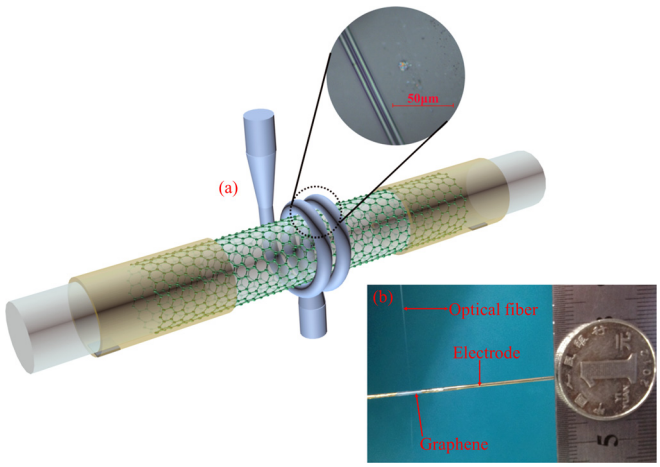

FIG. 1. (a) The schematic diagram of the graphene-based electrical current sensor. Inset shows a micrograph of the microfiber with the diameter of ~4.5 μm. The light yellow thin sheets coating around both ends of the graphene sheet are the Au electrodes. (b) Photo of the graphene-microfiber-integrated coil resonator, with a Chinese one yuan coin.

(PMMA). After the copper substrate is removed in the ferric chloride solution (1 mol/l), the graphene sheet is transferred onto the glass capillary rod and then the PMMA is dislodged by immersing the rod into the acetone solution. Finally, two Au electrodes are fabricated by depositing ~100 nm-thick Au film on both ends of the graphene sheet, as seen in Fig. 1(a). When the electrodes make contact with external current source, the electrical current can be loaded on the graphene sheet, which serves as a heater in the experiment. The waist region of the microfiber is approximately 1 cm, and the microfiber is wrapped around the graphene sheet with two turns to form a coil resonator. The diameter of the microfiber is ~4.5 μm, which can confine most of the mode field in the microfiber and avoid large loss from high refractive index of the silica rod. The diameter of the glass capillary rod is ~840 μm. Figure 1(b) shows the photo of the graphene-microfiber-integrated coil resonator.

The broadband amplified spontaneous emission (ASE) source (1525–1565 nm) and the optical spectrum analyzer (OSA, YOKOGAWA AQ6370C) are used to measure the output spectrum throughout the entire experiment. Pigtails of the microfiber are spliced into the light path. From the measured transmission spectrum shown in Fig. 2, the free spectral

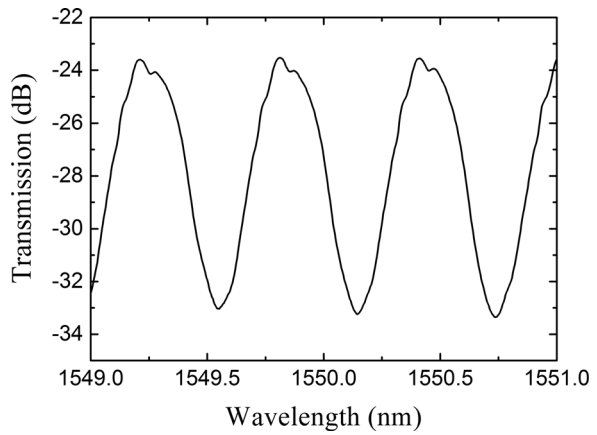

FIG. 2. The transmission spectrum of the microfiber coil resonator.

range (FSR) is about 0.6 nm, and the extinction ratio is approximately 10 dB. A wider FSR corresponds to a thinner glass capillary rod with the relation of $FSR \approx \lambda^2/\pi n_{eff} D$, where λ is the wavelength, n_{eff} is the effective refractive index, and D is the diameter of the rod, respectively. The extinction ratio of the spectrum can be adjusted by tuning the spacing of adjacent coils and the coil numbers wrapped around the rod.[19]

As for a coil resonator by a microfiber wrapping around a rod, the resonant condition can be expressed as

$$\frac{2\pi}{\lambda_{res}} \times n_{eff} \times L = 2m\pi, \tag{1}$$

where λ_{res} is the resonant wavelength, n_{eff} is the effective refractive index, L is the coil length, and m is an integer.

The current source meter (Keithley 2400) can provide a steady electrical current. When electrical current flows through the Au electrode, the monolayer graphene sheet, and another Au electrode, heat generates quickly because of the large sheet resistance of the monolayer graphene sheet. Enormous heat from the graphene sheet results in thermo-optic effect and thermal expansion effect on the microfiber coils. The refractive index and diameter of the microfiber change synchronously. Thus, the coupling between coils changes, and the resonant wavelength shifts with the temperature variation as the relation

$$\begin{aligned}\Delta\lambda &= \Delta\lambda_{TOE} + \Delta\lambda_{TEE} \\ &= \frac{\lambda_{res}}{n_{eff}} \times \left[\frac{\partial n_{eff}}{\partial n_{MF}} \times \sigma_{MF} + \left(n_{eff} + \frac{\partial n_{eff}}{\partial r_{MF}} \times r_{MF}\right) \times \alpha_{MF}\right] \\ &\quad \times \Delta T,\end{aligned} \tag{2}$$

where σ_{MF} and α_{MF} are the thermo-optic and thermal expansion coefficients of the microfiber, ΔT represents the temperature variation due to the heat, n_{MF} and r_{MF} are refractive index and radius of the microfiber, respectively. For silica microfiber, σ_{MF} is $1.1 \times 10^{-5}/^{\circ}\mathrm{C}$, and α_{MF} is $5.5 \times 10^{-7}/^{\circ}\mathrm{C}$.

The temperature variation can be expressed as

$$\Delta T \propto \frac{\rho l}{w} \times I^2, \tag{3}$$

where ρ, l, and w are the sheet resistivity, length, and width of the graphene sheet, respectively, and I represents the electrical current.

Thus, the relation between resonant wavelength shift and current variation can be expressed as

$$\frac{\Delta\lambda_{res}}{\lambda_{res}} \propto \frac{\rho l}{w} \times I^2. \tag{4}$$

Finally, the sensitivity of electrical current can be expressed as

$$S = \frac{\Delta\lambda}{I^2}. \tag{5}$$

The resistance is measured to be ~4.6 kΩ in the experiment, which consists of sheet resistance of the graphene sheet, sheet resistance of the metal, and contact resistance for metal-graphene interface.[23–26] Among them, the first

source of resistance is the major part. The length of the graphene sheet is ~5.5 mm, and the width is approximately the perimeter of the rod. The large sheet resistance of the graphene sheet is mainly on account of defects produced from transfer process of the graphene sheet to the rod.

We calculate the temperature variation on account of the change of square of electrical current with finite element method. In the simulation, we use the vertical section of the rod as a two-dimensional model due to its circular symmetry. The thickness is set as 840 μm, and the longitudinal length of the heat source (graphene) is 5.5 mm, with the heat flux set to be 311 W/m^2. The length of each electrode is 35 mm. Here, the heat transfer coefficient between the rod and air is 12 W/(m^2·K),[27] and the external temperature is 295 K. Due to the small heat transfer coefficient, heat generated from graphene sheet concentrates on the rod, and a large temperature variation arises. Thereto, the influence from the microfiber is negligible due to its small dimension compared with the rod. When the change of square of electrical current is 1 mA^2, temperature variation is approximately 8 °C. Thus, we can estimate the current sensitivity as 101.298 μm/A^2 by using Eqs. (2) and (5).

Figure 3 displays the transmission spectrum shifts with different electrical currents. The current-generating heat warms up the microfiber and redshifts the resonator wavelength. It can be seen that the current-generating heat in the graphene does not induce extra loss. Figure 4 shows the measured dip wavelength redshifts from 1549.552 nm to 1550.156 nm as a function of the square of electrical current ranging from 0 to 3 mA, in both ascending and descending directions. The results in ascending and descending directions keep good linearity and match well with each other, and the curves represent the linear fitting results for the experimental data with the varying square of electrical current. The average electrical current sensing sensitivity is around 67.297 μm/A^2, which is two orders of magnitude higher than other current sensors based on thermal effect described earlier.[9–13] As for the result by simulation and calculation is larger than the experimental result, we attribute the reasons to some approximations such as the neglect of contact resistance in the simulation and heat transfer coefficient of air in the process of simulation. We can decrease the contact resistance by increasing the contact width or changing the

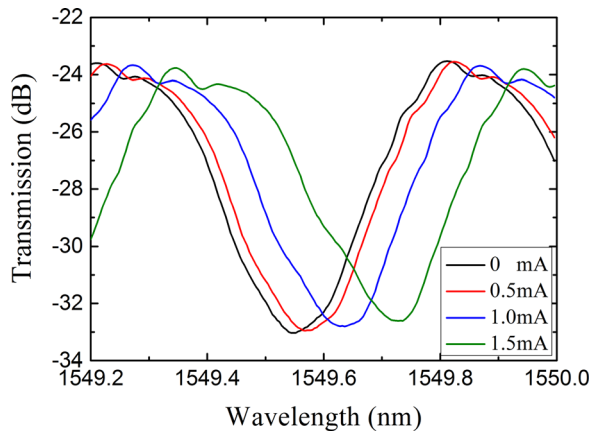

FIG. 3. Transmission spectrum shifts with different electrical currents.

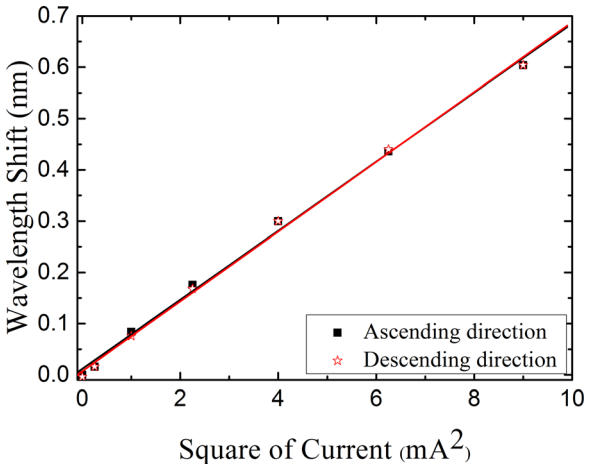

FIG. 4. Dip wavelength redshifts as a function of the square of electrical current ranging from 0 to 3 mA in both ascending and descending directions. The curves represent the linear fitting of the experimental data.

electrodes to be metal Ni in the experiment to improve the sensor's performance.[24] Utilizing other metallic films as electrodes such as Ni could be an option to reduce the contact resistance, but it remains to be demonstrated for the present device later. Due to the limit of thermal effect and the configuration, we can get a response time to be less than one and a half minutes. The sensor detection limit can be calculated as $(\delta\lambda/S)^{1/2}$, where $\delta\lambda$ is the smallest measurable wavelength shift assumed as one-twentieth of full width at half maximum of the resonance. From Fig. 2, the full width at half maximum can be estimated to be ~0.35 nm. Thus, the detection limit can be calculated as ~0.5 mA. Lower detection limit can be achieved with a larger sheet resistance of graphene and a smaller microfiber resonator.

It is very difficult to get the precise surface temperature variance due to the limit of measuring equipment. In our experiment, we utilize a thermocouple (TES-1310, Taiwan) to acquire the surface temperature. We find the temperature variance is $\sim 8 \times 10^{-4}$ °C/(Ω/□), when the current is 1 mA. The current sensitivity is ~22.4 μm/A^2, which is smaller than the experimental result due to the thermocouple whose dimension is relatively large (millimeter level).

Optical fiber current sensor based on thermal effect unavoidably induces some influences on the system under current test. Generally, the influence due to the sensor can be minimized or even compensated by use of signal processing methods. Shrinking the length of graphene sheet to be analogous with the height of microfiber coils (longitudinal direction of the rod) could minimize the energy waste of the device and keep the sensitivity level. On the other hand, to reduce the large resistance's impact on the system under test, adjusting the length-width ratio of the graphene sheet coated around the rod is an option. Besides, adding a parallel low resistance to reduce the whole resistance is another method with the cost of the reduction of the sensitivity. So we have to balance the trade-off between the influence and sensitivity in practical applications.

In this work, a graphene-based electrical current sensor is proposed utilizing a microfiber coiling around a glass capillary rod to form a resonator. The rod is coated by a monolayer graphene sheet in advance. The Au electrodes are

coated on both ends of the graphene sheet to conduct electrical current. Due to the large sheet resistance of graphene, the thermo-optic effect and thermal expansion effect shift the resonant wavelength of the microfiber coil resonator. Based on the graphene-microfiber-integrated coil resonator, the sensor shows an ultra-high sensitivity, which is two orders of magnitude higher than current sensors based on thermal effect described earlier.[9–13] Moreover, the sensor shows a good repeatability.

This work was sponsored by National 973 Program (Nos. 2012CB921803 and 2011CBA00205) and National Natural Science Foundation of China (Nos. 61322503, 61225026, and 61475069).

[1]B. Lee, Opt. Fiber Technol. **9**, 57 (2003).
[2]M. Belal, Z. Song, Y. Jung, G. Brambilla, and T. P. Newson, Opt. Lett. **35**, 3045 (2010).
[3]G. Y. Chen, T. Lee, R. Ismaeel, G. Brambilla, and T. P. Newson, IEEE Photonics Technol. Lett. **24**, 860 (2012).
[4]G. Y. Chen, G. Brambilla, and T. P. Newson, Electron. Lett. **48**, 1547 (2012).
[5]S. Qiu, Q. Liu, F. Xu, and Y. Lu, Sens. Actuators, A **210**, 95 (2014).
[6]M. Belal, Z. Song, Y. Jung, G. Brambilla, and T. Newson, Opt. Express **18**, 19951 (2010).
[7]A. A. Jasim, S. W. Harun, M. Z. Muhammad, H. Arof, and H. Ahmad, Sens. Actuators, A **192**, 9 (2013).
[8]K. Ramachandran, N. Kumar, and V. Sahoo, IEEE Sens. J. **15**, 1270 (2015).
[9]K. S. Lim, S. W. Harun, S. S. A. Damanhuri, A. A. Jasim, C. K. Tio, and H. Ahmad, Sens. Actuators, A **167**, 60 (2011).
[10]A. Sulaiman, S. W. Harun, I. Aryanfar, and H. Ahmad, Electron. Lett. **48**, 943 (2012).
[11]A. Sulaiman, S. W. Harun, F. Ahmad, S. F. Norizan, and H. Ahmad, IEEE J. Quantum Electron. **48**, 443 (2012).
[12]G. Y. Chen, G. Brambilla, and T. P. Newson, Electron. Lett. **49**, 46 (2013).
[13]X. Xie, J. Li, L. Sun, X. Shen, L. Jin, and B. Guan, Sensors **14**, 8423 (2014).
[14]A. K. Geim, Science **324**, 1530 (2009).
[15]S. Chen, L. Brown, M. Levendorf, W. Cai, S. Ju, J. Edgeworth, X. Li, C. W. Magnuson, A. Velamakanni, R. D. Piner, J. Kang, J. Park, and R. S. Ruoff, ACS Nano **5**, 1321 (2011).
[16]F. Schedin, A. K. Geim, S. V. Morozov, E. W. Hill, P. Blake, M. I. Katsnelson, and K. S. Novoselov, Nat. Mater. **6**, 652 (2007).
[17]Y. Shao, J. Wang, H. Wu, J. Liu, I. A. Aksay, and Y. Lin, Electroanalysis **22**, 1027 (2010).
[18]I. M. Rycroft and B. L. Evans, Thin Solid Films **290–291**, 283 (1996).
[19]G. Brambilla, J. Opt. **12**, 043001 (2010).
[20]G. Brambilla, F. Xu, P. Horak, Y. Jung, F. Koizumi, N. P. Sessions, E. Koukharenko, X. Feng, G. S. Murugan, J. S. Wilkinson, and D. J. Richardson, Adv. Opt. Photonics **1**, 107 (2009).
[21]J. Kou, J. Chen, Y. Chen, F. Xu, and Y. Lu, Optica **1**, 307 (2014).
[22]G. Brambilla, V. Finazzi, and D. J. Richardson, Opt. Express **12**, 2258 (2004).
[23]Y. Matsuda, W. Deng, and W. A. Goddard, J. Phys. Chem. C **114**, 17845 (2010).
[24]K. Nagashio, T. Nishimura, K. Kita, and A. Toriumi, Appl. Phys. Lett. **97**, 143514 (2010).
[25]S. M. Song, T. Y. Kim, O. J. Sul, W. C. Shin, and B. J. Cho, Appl. Phys. Lett. **104**, 183506 (2014).
[26]S. Russo, M. F. Craciun, M. Yamamot, A. F. Morpurgo, and S. Tarucha, Physica E **42**, 677 (2010).
[27]V. S. Arpaci, A. Selamet, and S. Kao, *Introduction to Heat Transfer* (Prentice Hall, New Jersey, 2000), p. 22.